

40-W CW Broad-Band Spatial Power Combiner Using Dense Finline Arrays

Nai-Shuo Cheng, *Student Member, IEEE*, Angelos Alexanian, *Member, IEEE*, Michael G. Case, *Senior Member, IEEE*, David B. Rensch, and Robert A. York, *Senior Member, IEEE*

Abstract— This paper presents a broad-band spatial power-combining system based on tapered-slot antenna arrays integrated in a standard WR-90 waveguide environment. The system is designed using a modular tray architecture, providing full waveguide-band frequency coverage and an excellent thermal environment for a set of monolithic-microwave integrated-circuit (MMIC) amplifiers. The shape of the tapered-slot or finline structures was optimized to minimize return loss and provide a broad-band impedance transformation from the waveguide mode to the MMIC amplifiers. A prototype eight-element array using commercial GaAs MMIC power amplifiers yielded a maximum of 41-W output power (continuous wave) with a gain variation less than ± 1.2 dB within the entire band of interest. The average combining efficiency over the operating band was estimated at 73%. The results suggest the efficacy of the design and a strong potential for higher powers by moving toward a greater number of MMIC's per tray and a larger number of trays. Should the 100-W system be realized in the near future, our combiner system will become a promising candidate to challenge the dominant position currently claimed by the traveling-wave tube amplifiers.

Index Terms— Finline structure, power combining, spatial power combiner.

I. INTRODUCTION

HIGH-POWER amplifiers are a necessary component of wireless transmitters at microwave and millimeter-wave frequencies. Solid-state amplifiers have desirable characteristics, but are generally unavailable at high-power levels and/or broad bandwidths, forcing systems designers to use vacuum-tube devices. This has motivated research activities in the area of spatial power combining or multiple solid-state amplifiers [1]. Many circuit-level combining approaches, such as corporate combining, suffer from increased loss (and, hence, reduced combining efficiency) as the number of devices increases. On the contrary, loss is relatively independent of the number of devices in a well-designed spatial combiner. As a result, spatial power combining is favored in certain high-power applications requiring a large number of amplifiers [2].

Manuscript received September 15, 1998. This work was supported in part by the Defense Advanced Research Projects Agency Microwave and Analog Front End Technology Program under Contract N66001-96-C-8625 and in part by the Office of Naval Research Multidisciplinary Research Program for the University Research Initiative Program under Grant N00014-96-1-1215.

N.-S. Cheng and R. A. York are with the Electrical and Computer Engineering Department, University of California at Santa Barbara, Santa Barbara, CA 93106 USA.

A. Alexanian is with the Research and Development Group, AMP/M/A-COM, Lowell, MA 01853-3294 USA.

M. G. Case and D. B. Rensch are with HRL Laboratories, Malibu, CA 90265-4737 USA.

Publisher Item Identifier S 0018-9480(99)05299-0.

For the implementation of high-power spatial combiners, where the output power is at the level of tens or hundreds of watts, several issues have to be incorporated in the design to achieve the desired performance. When dealing with a large number of high-power amplifiers, thermal management is extremely important since device performance degrades drastically if waste heat cannot be removed efficiently. The combiner must be compact, but large enough (physically and thermally) to accommodate the desired number of amplifiers. Minimizing output combiner losses is also critical as far as combiner efficiency is concerned. It is worth emphasizing that for combiner systems based on high-gain amplifiers, only the loss associated with the output network is important [2]. A well-designed combiner should ideally exhibit broad-band characteristics, i.e., a frequency-independent $50\text{-}\Omega$ impedance environment so that the performance of the individual (isolated) monolithic-microwave integrated-circuit (MMIC) amplifiers can be retained. In this way, the combiner system is also technology independent, requiring only that the MMIC's are unconditionally stable inside of the desired operating band.

In a previous paper, we reported a new waveguide-based spatial power-combiner circuit that addressed these issues [3]–[5]. The concept is illustrated schematically in Fig. 1(a); we exploit the inherent spatial distribution of the field energy in the dominant waveguide mode to distribute and collect power to and from a dense array of amplifiers. Transitions between the amplifier and waveguide mode are made via electrically close tapered-slot antennas (or finline structures). The enclosed waveguide provides an excellent heat-sinking environment for the power devices and is a natural choice for most high-power applications.

In this paper, we present the design and fabrication of a new version of a spatial power combiner, as illustrated in Fig. 1(b), which is based on the same operating principle, but provides solutions to many problems encountered in the previous design. Efforts have been devoted to further improvements on heat sinking, characterization, and optimization of passive waveguiding structures, integration of high-performance MMIC amplifiers, and enhancement of overall system design.

II. CIRCUIT DESIGN

The prototype spatial combiner was implemented by using a 2×4 array of active devices, integrated with input/output antenna arrays in a standard X -band waveguide environment. This design was to serve as a proof-of-concept toward an ultimate goal of a $>100\text{-W}$ combiner system at X -band.

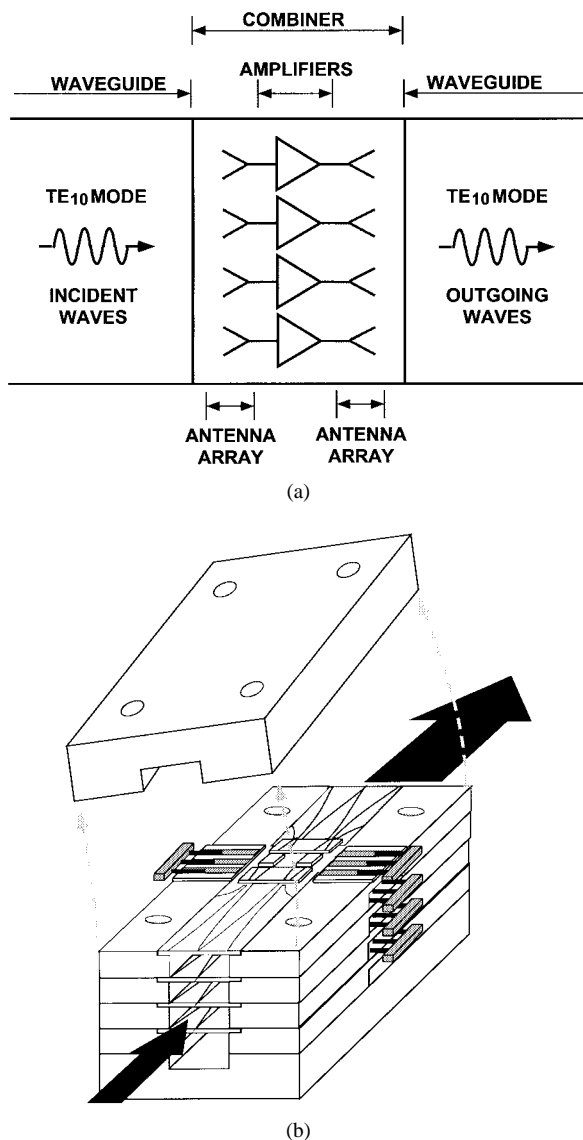


Fig. 1. (a) Schematic diagram. (b) Graphical illustration of the operating principle of the combiner circuit.

Fig. 2 shows the schematic plot of the test fixture, which forms the main body of the combiner circuit. It adopts a modular tray architecture, which makes the packaging compact and assembling straightforward. The fixture consists of four identical trays, along with the top/bottom covers and a base plate. The completely enclosed structure eliminated radiation loss in the system, a problem which plagued earlier designs [2]–[4]. The prototype designs were constructed from aluminum for ease of fabrication; however, copper will be used for the future high-power systems.

Each “H”-shaped tray was designed to accommodate separate input and output “antennas,” which rest in grooved channels so that the antenna surface is flush with the tray surface. The MMIC’s and associated radio-frequency (RF) feed and dc bias circuitry were mounted directly onto the metal crossbar of the tray. Bondwires were used to make connections between antennas and MMIC amplifiers, resulting in a crude, but effective slotline-to-microstrip transition.

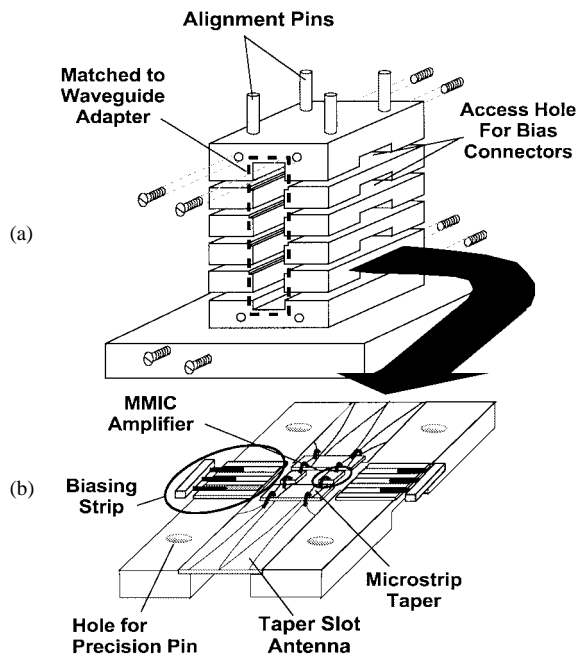


Fig. 2. (a) Schematic plot of the test fixture. (b) Layout on a single tray.

When all the components are stacked and bolted together, two WR-90 waveguide apertures are formed at the input and output ends of the test fixture. Alignment pins were used to hold the fixture in exact position. At each side of the test fixture there are notched openings on each tray, which allow for distribution of dc bias to the MMIC amplifiers from an external power supply.

Tapered slot antennas are broad band in nature and, therefore, attractive for this combiner system. 10-mil-thick aluminum nitride (AlN) substrates with single-sided metallization were used to realize the antennas. By using standard photolithographic processes, the antenna pattern was defined and etched in a 3.4- μm -thick gold layer. The taper shape of the finline structure was optimized to minimize the return loss and provide appropriate impedance transformation from the waveguide to the MMIC amplifiers (see Section III).

The commercially available MMIC GaAs power amplifiers used in this work were individually attached to a heat-spreader by the manufacturer using vacuum-reflow eutectic soldering techniques. These MMIC’s were subsequently attached directly onto the test fixture using conducting silver epoxy. This arrangement provided for dissipation of approximately 150-W of dc power with a 41 °C rise above the ambient at the base of the MMIC’s. Note that more MMIC amplifiers can be laterally added to the space adjacent to the existing amplifiers. In addition, the number of trays could also be increased so that more active elements can be integrated into the combiner circuit. The number of trays is ultimately limited by the waveguide aperture and the minimum achievable thickness of the trays, as well as by thermal management.

III. OPTIMAL TAPER DESIGN

In order to minimize the return loss of the taper slot antenna arrays, the shape of the taper structure has to be properly

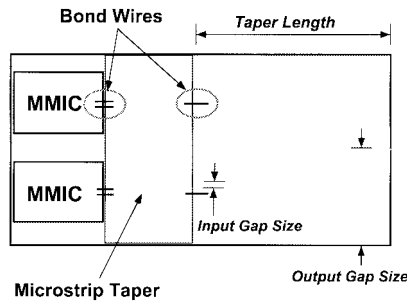


Fig. 3. Shape of the taper slot antenna structure has to be determined to minimize return loss and provide proper impedance transformation between MMIC amplifiers and the waveguide.

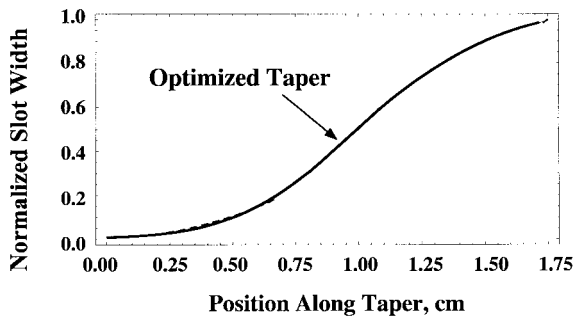
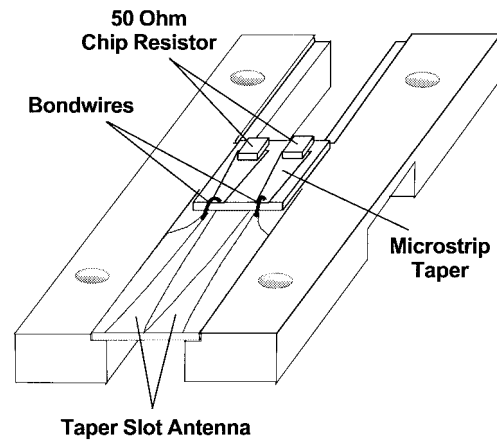


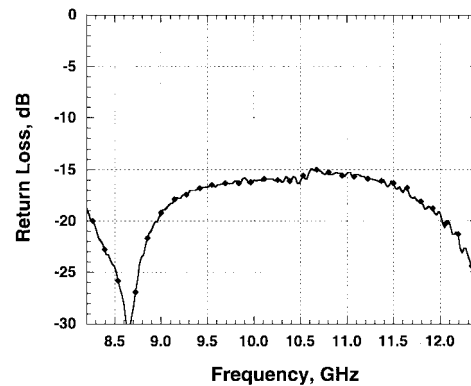
Fig. 4. The taper shape was optimized and determined. The plot shows the relationship between the (normalized) gap width and the position along the taper.

designed. Klopfenstein developed similar “optimal tapers” for TEM structures based on the theory of small reflections [6]. These designs specify the impedance value at each point along the taper in order to achieve a specified maximum allowable return loss in the passband. With proper modification (using wave impedances instead of characteristic impedances), the original design concept can be extended and applied to non-TEM waveguiding structures [7]. Finlines operate in a quasi-TE mode, where the longitudinal electric-field component is negligible when compared to the transverse components. This knowledge establishes an important link between the propagation constants (which can be easily computed) and the wave impedance.

Fig. 3 shows the schematic plot of a single antenna card, which outlines the design problem of interest. Before the optimal tapered structure can be designed, both the gap sizes at the input and output ends of the taper have to be specified, along with the taper length and required maximum return loss. The output gap size was set by the size of the waveguide opening and the number of antennas. Ideally, we would like to choose the input gap size so that the MMIC amplifier could see a $50\text{-}\Omega$ environment; however, it was practically impossible to do that in this particular case. At an input gap size of $52\text{ }\mu\text{m}$, the slotline characteristic impedance was found to be approximately $100\text{ }\Omega$. Therefore, an additional microstrip taper was designed and incorporated into the existing circuitry to serve as an $100\text{--}50\text{-}\Omega$ impedance transformer. The microstrip carrier was mounted on the tray much like the MMIC amplifiers, and were also used to carry bias to the innermost reaches of the tray.



(a)



(b)

Fig. 5. (a) Test circuit and (b) results for the return-loss measurements for a 2×2 system, with the end of microstrip taper terminated with $50\text{-}\Omega$ chip resistor.

Once the input and output gap sizes were determined, the wave impedance along the position of the taper line could be derived from the design equations that apply to non-TEM structures [7]. In order to realize the physical layout of the optimal taper, the relationship between the propagation constants and geometric parameters of the finline array then had to be established. The spectral-domain method [8] was used to set up integral equations, which were then solved by the method of moments. Consequently, under the assumption of TE operation for finlines, the corresponding slot width to specific wave impedance, which is a function of the propagation constant, could be determined. Fig. 4 shows the resulting optimized taper shape for the structure, with a design goal of return loss better than -20 dB for the entire operating band of $8\text{--}11\text{ GHz}$.

Return-loss measurements were performed to verify the taper design for a 2×2 system. The test circuit is shown in Fig. 5(a), where the end of the microstrip taper is terminated with a $50\text{-}\Omega$ chip resistor. The measured return loss shown in Fig. 5(b) was better than -15 dB for the entire waveguide band, which was sufficiently close to the design goal for this work. It is worth noting that theoretically there is no upper limit for the bandwidth of the gradual taper and, therefore, the bandwidth is currently limited by the waveguide and MMIC amplifiers.

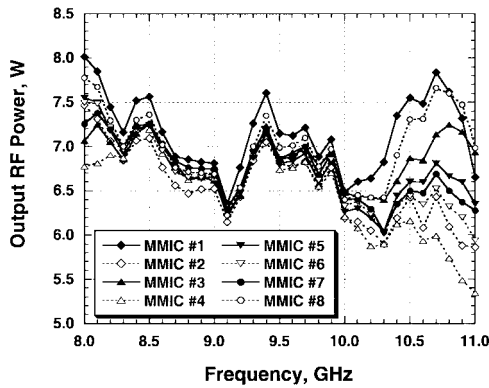


Fig. 6. Power measurements for individual MMIC amplifiers. Output power was measured when incident RF power was 21 dBm. The plot is shown on a linear scale.

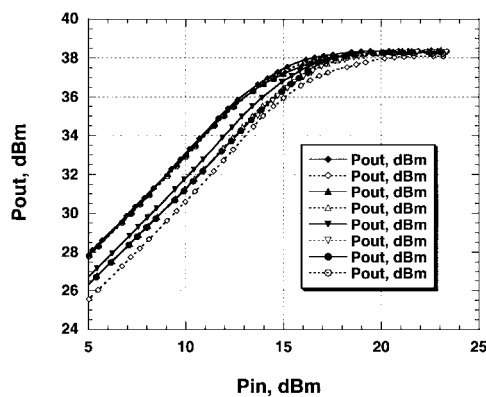


Fig. 7. P_{out} versus P_{in} measurements for individual MMIC amplifiers.

IV. MMIC POWER AMPLIFIERS

The MMIC amplifiers used in this work were commercially available parts from the TGA9083-EEU, Texas Instruments Incorporated (now TriQuint-TI), Dallas, TX. The amplifiers were mounted on individual carriers for better handling and easy attachment. External bias capacitors were epoxy-mounted onto the test fixture in close proximity to the MMIC amplifiers for low-frequency stabilization. Gold wires with 1-mil diameter were used for electrical connections for both RF and dc purposes. Careful attention was paid during the assembly process in minimizing bondwire lengths and avoiding potential electrical shorting of components due to excessive epoxy.

The nominal specifications for this MMIC amplifier was 8-W continuous wave (CW) at 9-V drain bias over the range of 6.5–11 GHz, with a small-signal gain of 19 dB and power-added efficiency (PAE) of 33%–40%. On-chip active gate biasing was used to simplify the biasing setup. Each MMIC amplifier was characterized in isolation for performance screening and bias setup. Fig. 6 shows a plot of output RF power versus frequency (linear scale) for the MMIC's used in this work. Fig. 7 illustrates the output power versus input power measurements at 9 GHz, showing some differences in saturated power and linear gain among MMIC amplifiers. On average, the actual maximum output RF power from a single MMIC was approximately 6.9 W when driven into saturation.

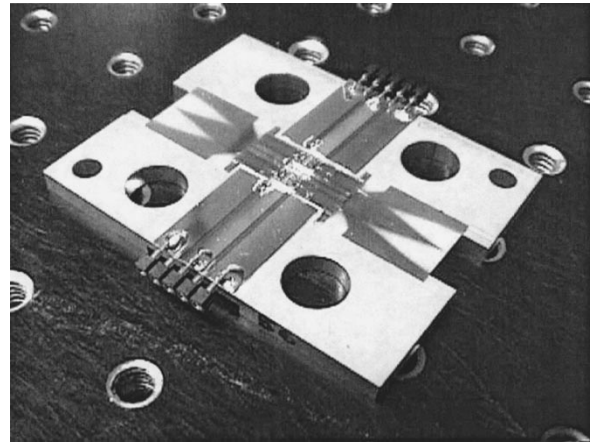


Fig. 8. Photograph of the overview circuit layout on a single tray.

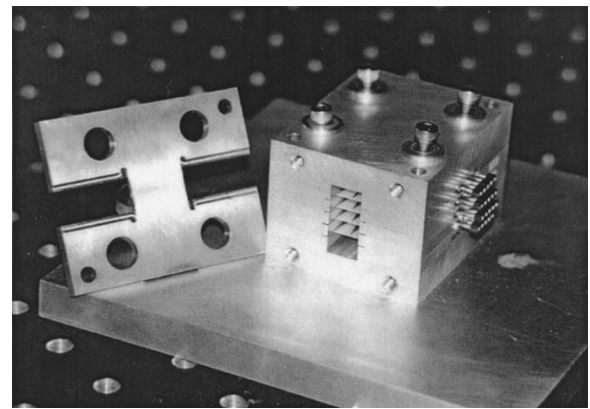


Fig. 9. Photograph of the combiner circuit based on 2×4 arrays.

V. COMBINER PERFORMANCE

A finished tray and the assembled four-tray combiner system are shown in Figs. 8 and 9. CW power measurements were performed using the measurement setup illustrated in Fig. 10. Coaxial-to-waveguide adapters were used to create a coaxial-based environment for measurements. A traveling-wave tube (TWT) amplifier, along with a sweeper, was utilized to generate an input RF signal of approximately 30 dBm. A 20-dB attenuator was placed directly after the output adapter to bring down the output power level and prevent the power sensor from receiving excessive power. At the input, a directional coupler was used to sample the input power level, while at the output, the other coupler was employed to monitor the output RF signal with a spectrum analyzer. Measurement data were taken up to 11 GHz, where the performance of MMIC amplifiers starts to degrade.

A maximum output power of about 41 W was observed at 8.7 GHz, with a corresponding gain of about 16.5 dB, as shown in Fig. 11. The gain varies within the range from 13.8 to 16.5 dB, indicating a remarkably broad-band characteristic, with only less than ± 1.4 -dB gain variation. The PAE of the combiner circuit fluctuates, in the range from 17% to 27%, as the frequency varies. About 150 W of dc power and 17 A of drain current by average were consumed by a total of eight MMIC amplifiers when the combiner was in operation.

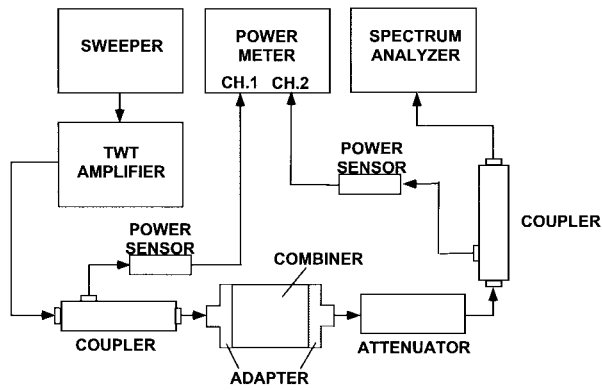


Fig. 10. Power measurement setup.

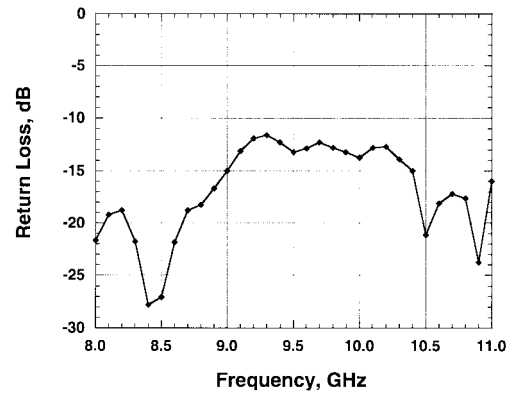


Fig. 12. Return-loss property of the combiner circuit.

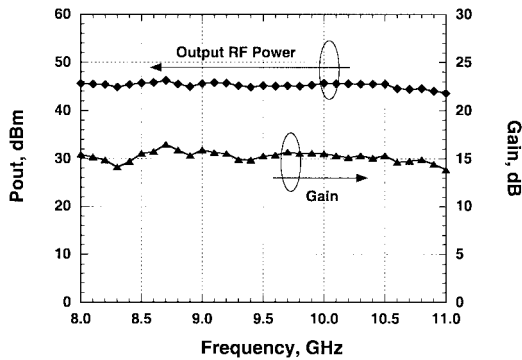
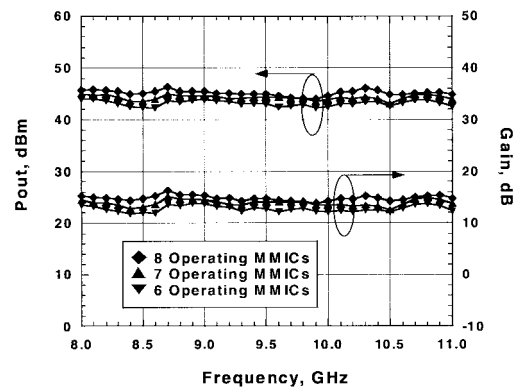
Fig. 11. Power measurements for the combiner circuit. $P_{in} = 30$ dBm.

Fig. 13. Graceful degradation characteristic of the combiner circuit.

Thermocouples were used and attached to various positions on the body of test fixture for temperature measurement. Approximately 41°C of temperature difference existed between the bottom surface of the metal carrier directly underneath the MMIC amplifiers and the base plate, which was about 25°C . These numbers suggest that the MMIC amplifiers were operated under a benign condition and the waste heat has been efficiently removed during the measurements.

The return-loss characteristic for the combiner circuit, as shown in Fig. 12, is better than -10 dB for the entire frequency band. It can be seen that Figs. 6 and 12 both show results with similar shaped curves, indicating that the combiner circuit presents a consistent return-loss characteristic, as was seen in the passive/tapered structure. The graceful degradation property of the combiner is shown in Fig. 13. Two MMIC amplifiers, located on two outer trays, were intentionally turned off to examine the corresponding effect on the power performance. No catastrophic failure or resonant dips were observed as a result of the loss of these amplifiers. The output power and gain gradually reduce when the number of operating MMIC amplifiers decreases; however, the combiner lost about 19% and 37% of original output power, respectively, for the cases when one and two MMIC amplifiers were turned off. Ideally, this would be 12.5% and 25% if the devices were perfectly isolated.

VI. INFLUENCE OF NONUNIFORM FIELD PROFILE

Since the waveguide operates in the dominant TE_{10} mode, there is a nonuniform excitation of the trays. The MMIC

amplifiers that are located close to the center of the waveguide receive more incident RF power than the ones at the outer positions. This should lead to some degradation in output power for a given input power, especially when MMIC amplifiers operate in or near saturation, which, in turn, affects the combining efficiency and PAE. However, it is difficult to quantify this analytically without detailed electromagnetic analysis.

To begin to address the issue experimentally, measurements were made using a two-tray combiner system. In this case, each MMIC amplifier should receive the same amount of incident RF power, and an accurate estimate of combining efficiency can be made using earlier measurements of the individual MMIC performance. The combining efficiency is shown in Fig. 14, calculated by dividing the actual saturated power from the combiner by the total saturated power from all the MMIC amplifiers. The averaged combining efficiency is approximately 77%. Since this is essentially a measure of output losses in each tray, this number sets an upper limit on the combining efficiency of the four-tray system.

The effect of the nonuniform illumination in the four-tray system was examined using a simple calculation. We assume eight identical MMIC amplifiers, each generating 7 W of saturated power and 20 dB of linear gain, which approximates our actual MMIC's. The saturation characteristics were then modeled by [9]

$$P_{\text{OUT},i} = P_{\text{SAT},i} \left(1 - \exp \frac{-P_{\text{IN},i} G_i}{P_{\text{SAT},i}} \right) \quad (1)$$

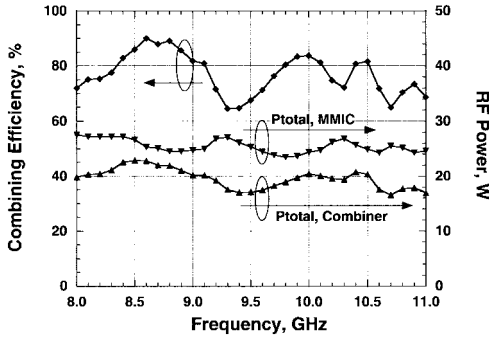
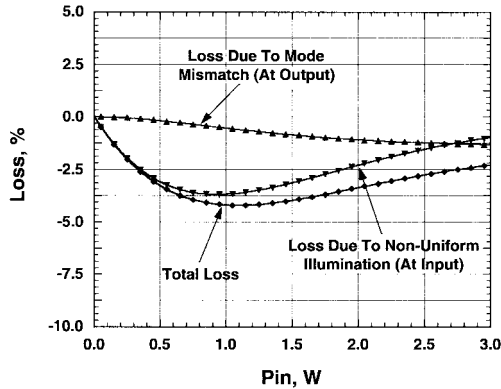

 Fig. 14. Combining efficiency of the combiner circuit, based on 2×2 arrays.


Fig. 15. Losses due to mode mismatch and nonuniform illumination.

where $P_{OUT,i}$, $P_{SAT,i}$, $P_{IN,i}$, and G_i represent the output power, saturated power, input power, and linear gain, respectively, for the i th MMIC amplifier in the combiner circuit. The input power to each MMIC was estimated by assuming a TE_{10} -mode excitation and accounting for the location of each tray in the waveguide. Based on these assumptions, it was calculated that the two center trays jointly receive approximately 67% of the total incident power, while the two outer trays jointly receive approximately 33% of the total incident power.

The total output power can be calculated by summing up all the output power from each MMIC amplifier

$$P_{OUT} = \sum_{i=1}^8 P_{OUT,i}. \quad (2)$$

The percentage of loss in available power was calculated by using

$$LOSS = \frac{P_{OUT,Uniform} - P_{OUT,non-uniform}}{P_{OUT,Uniform}} \quad (3)$$

and is shown in Fig. 15. Somewhat surprisingly, the loss peaks at only -3.8% at $P_{in} = 0.95$ W, suggesting that the nonuniform field distribution of the incident RF power does not seriously impact the RF power level available from the MMIC amplifiers in this particular combining structure. This is a result of clustering the cards toward the center of the waveguide.

We also need to consider the coupling loss caused by the mismatch between the waveguide-mode profile and the output

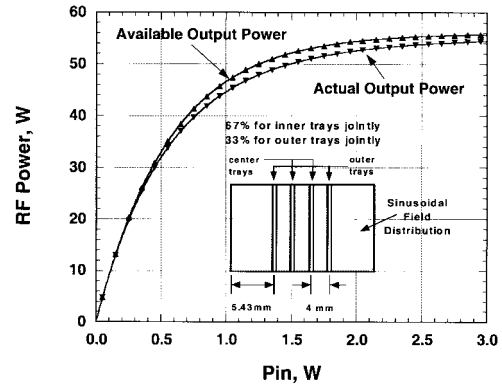


Fig. 16. Effect of nonuniform illumination of incident power on output power. The inset plot outlines the actual positions of the trays and each supports two MMIC amplifiers. Sinusoidal field distribution is assumed for the nonuniform case.

field distribution from the MMIC amplifiers. This effect is important only when the MMIC amplifiers operate in or near saturation. The coupling factor between two mode profiles can be calculated based on the following expression:

$$\eta = \iint \phi \psi ds \quad (4)$$

The output field distribution, calculated by using (1), (2), and the waveguide-mode profile, shown in the inset of Fig. 16, are represented by ϕ and ψ , respectively. Both ϕ and ψ were normalized, and the integration was performed over the entire waveguide cross section. The estimated coupling loss was derived as shown in Fig. 14. It can be seen that the coupling loss increases as the incident RF power increases. The coupling loss peaks at -1.3% ($P_{in} = 3$ W) where all the MMIC amplifiers saturate and each outputs the same amount of power. The total loss, accounting for losses due to mode mismatch and nonuniform illumination, is approximately -4.2% at $P_{in} = 1$ W. Fig. 15 shows the curves for available power from the MMIC's and the actual power coupled to the waveguide. At $P_{in} = 1$ W, the available power was 46.6 W and the actual power was 44.6 W, with a loss of approximately 2 W, or 4.2% of available power.

Combining the measured results from the two-card system (Fig. 13), which describes the power loss due to losses in the system, along with the estimate of power loss due to the nonuniform field profile and mismatch of mode profile (Fig. 15), we, therefore, estimate an average combining efficiency of approximately 73% for the four-tray combiner. The dominant loss mechanism is clearly ohmic and/or transition losses, and only a small part is related to the nonuniform field profile. This could apparently be increased through improved design of the transitions between the MMIC and antenna.

VII. CONCLUSION

We present a maximum 41-W (CW) result for a spatial combiner circuit based on eight commercial GaAs MMIC power amplifiers, integrated with 2×4 tapered finline arrays. Broad-band characteristics were achieved with a gain variation less than ± 1.4 dB covering the band from 8 to 11 GHz. The

average combining efficiency was estimated to be approximately 73%. It is worth mentioning that the resulting PAE and bandwidth of the combiner circuit were primarily limited by the MMIC amplifiers. The combining structure itself was quite efficient and broad band. The results suggest the efficacy of the design and a strong potential for higher powers by moving toward a greater number of MMIC's per tray and a larger number of trays. Should the 100-W system be realized in the near future, our combiner system will become a promising candidate to challenge the dominant position currently claimed by the TWT amplifiers. A patent has recently been issued to the University of California regarding this invention [5].

ACKNOWLEDGMENT

The authors would like to acknowledge the gracious support of Texas Instruments Incorporated, Dallas, TX, who provided the MMIC amplifiers, and Teledyne Electronic Technologies, Mountain View, CA, for their assistance in circuit assembly.

REFERENCES

- [1] M. A. Gouker, "Spatial power combining," in *Active and Quasi-Optical Arrays for Solid-State Power Combining*, R. A. York and Z. B. Popovic, Eds. New York: Wiley, 1997.
- [2] N.-S. Cheng, A. Alexanian, M. G. Case, and R. A. York, "20-W spatial power combiner in waveguide," in *IEEE MTT-S Int. Microwave Symp. Dig.*, Baltimore, MD, June 8–12, 1998.
- [3] A. Alexanian and R. A. York, "Broad-band waveguide-based spatial combiner," in *IEEE MTT-S Int. Microwave Symp. Dig.*, Denver, CO, June 8–13, 1997.
- [4] ———, "Broad-band spatially combined amplifier array using tapered slot transitions in waveguide," *IEEE Microwave Guided Wave Lett.*, vol. 7, pp. 42–44, Feb. 1997.
- [5] ———, "Waveguide-based spatial power combining array and method for using the same," U.S. Patent 5 736 908, April 7, 1998.
- [6] R. W. Klopfenstein, "A transmission-line taper of improved design," *Proc. IRE*, vol. 442, pp. 31–35, Jan. 1956.
- [7] N.-S. Cheng and R. A. York, "Analysis and design of tapered finline arrays for spatial power combining," in *IEEE AP-S Int. Symp. Dig.*, Atlanta, GA, June 21–28, 1998.
- [8] T. Itoh, "Spectral-domain immittance approach for dispersion characteristics of generalized printed transmission lines," *IEEE Trans. Microwave Theory Tech.*, vol. MTT-28, pp. 733–736, July 1980.
- [9] G. D. Vendelin, A. M. Pavio, and U. L. Rohde, *Microwave Circuit Design Using Linear and Nonlinear Techniques*. New York: Wiley, 1990, ch. 6.



Nai-Shuo Cheng (S'96) received the B.S. degree in nuclear engineering from National Tsing Hua University, Hsinchu, Taiwan, R.O.C., in 1989, the M.S.E.E. degree in electrical engineering from Syracuse University, Syracuse, NY, in 1994, and is currently working toward the Ph.D. degree in electrical engineering in the Electrical and Computer Engineering Department, University of California at Santa Barbara.

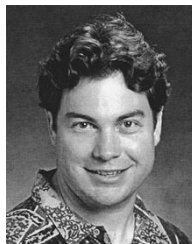
His current research involves the development of waveguide-based spatial power-combiner circuits and study of the propagation characteristics for non-TEM waveguiding structure by using the finite-difference method.

Mr. Cheng received second place in the Student Paper Competition at the 1998 IEEE International Microwave Theory and Techniques Society (MTT-S) Symposium.



Angelos Alexanian (S'92–M'93) was born in Athens, Greece, in 1968. He received the B.S. degree in electrical engineering (*summa cum laude*) from Virginia Polytechnic Institute and State University, Blacksburg, the M.S. degree in electrical engineering from The University of Michigan at Ann Arbor, in 1993, and the Ph.D. degree in electrical engineering from the University of California at Santa Barbara, in 1997.

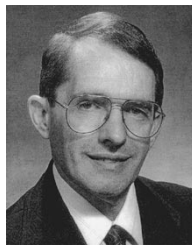
His research interests have included, time-domain analysis of periodic structures and power-combining schemes for broad-band high-power signal generation at microwave and millimeter-wave frequencies. Since August 1997, he has been with the Research and Development Group, AMP-M/A-COM, Lowell MA, where he is currently involved in the design, development, and production of 77-GHz radar sensors for automotive adaptive cruise control.



Michael G. Case (S'88–M'91–SM'98) was born in Ventura, CA, in 1966. He received B.S., M.S., and Ph.D. degrees from the University of California at Santa Barbara (UCSB), in 1989, 1991, and 1993, respectively.

In 1989, he began research at UCSB, where he studied nonlinear transmission lines for applications in high-speed waveform shaping and signal detection. Since 1993, he has been with HRL Laboratories, Malibu, CA, where he is currently involved with millimeter-wave device characterization, circuit design, and measurement techniques.

Dr. Case was the recipient of a state fellowship.



David B. Rensch received the B.E.E., M.S., and Ph.D. degrees in electrical from Ohio State University, Columbus, in 1964, 1965, and 1969, respectively.

Since 1969, he has been with HRL Laboratories, Malibu, CA, where he is currently the Manager of the Microwave Technology Department that conducts research and development into microwave technology associated with antennas, transmitter modules, and tunable filters associated with radar and communication systems. While with HRL Laboratories, he has been active in various technical areas, including gas lasers, focused ion beams in processing of microelectronics, high-temperature superconducting devices, and InP heterojunction bipolar transistor (HBT) power amplifiers.



Robert A. York (S'85–M'89–SM'99) received the B.S. degree in electrical engineering from the University of New Hampshire, Durham, in 1987, and the M.S. and Ph.D. degrees in electrical engineering from Cornell University, Ithaca, NY, in 1989 and 1991, respectively.

He is currently an Associate Professor in the Electrical and Computer Engineering Department, University of California at Santa Barbara (UCSB), where his group is currently involved with the design and fabrication of novel microwave and millimeter-wave circuits, microwave photonics, high-power microwave and millimeter-wave modules using spatial combining and wide-bandgap semiconductor devices, and application of ferroelectric materials to microwave and millimeter-wave circuits and systems.

Dr. York received the 1993 Army Research Office Young Investigator Award and the 1996 Office of Naval Research Young Investigator Award.